

FACM: Correct the Output of Deep Neural Network with Middle Layers Features against Adversarial Samples

Xiangyuan Yang, Jie Lin, Hanlin Zhang, Xinyu Yang, and Peng Zhao

Abstract—In the strong adversarial attacks against deep neural network (DNN), the output of DNN will be misclassified if and only if the last feature layer of the DNN is completely destroyed by adversarial samples, while our studies found that the middle feature layers of the DNN can still extract the effective features of the original normal category in these adversarial attacks. To this end, in this paper, a middle Feature layer Analysis and Conditional Matching prediction distribution (FACM) model is proposed to increase the robustness of the DNN against adversarial samples through correcting the output of DNN with the features extracted by the middle layers of DNN. In particular, the middle Feature layer Analysis (FA) module, the conditional matching prediction distribution (CMPD) module and the output decision module are included in our FACM model to collaboratively correct the classification of adversarial samples. The experiments results show that, our FACM model can significantly improve the robustness of the naturally trained model against various attacks, and our FA model can significantly improve the robustness of the adversarially trained model against white-box attacks with weak transferability and black box attacks where FA model includes the FA module and the output decision module, not the CMPD module.

Index Terms—Adversarial samples, correction model, diversity property, deep neural network.

I. INTRODUCTION

Deep neural networks (DNN) were shown to be susceptible against adversarial examples: adversarial perturbed samples will cause mis-classification while being nearly “imperceptible”, i.e., very close to the original samples. Ding et al. [1] has explored that the added imperceptible noise of the input will be amplified layer by layer till the output layer makes a wrong classification. However, the noise generated by white-box attacks with weak transferability (e.g., CW_∞ [2], CW_2 [2] and DeepFool L2 [3]) may just destroy the output layer of DNN to make a wrong classification, while the output of the middle layers of DNN still contains the correct features of the original category. Hence, the features extracted by the middle layers of DNN can be used to correct the output of the DNN against adversarial samples generated by white-box attacks with weak transferability.

Adversarial training (AT) is currently one of the most effective defenses against adversarial attacks for deep learning models. Various variants of adversarial training methods are proposed. For example, Adversarial Training with Hypersphere Embedding (ATHE) [4], Fast Adversarial Training (Fast-AT) [5], Friendly Adversarial Training (FAT) [6], Adversarial Training with Transferable Adversarial examples (ATTA) [7], You Only Propagate Once (YOPO) [8], Fair-Robust-Learning (FRL) [9], TRadeoff-inspired Adversarial DEfense via Surrogate-loss minimization (TRADES) [10] were proposed to enhance the robustness of DNN. However, these adversarial training methods focused on accelerating adversarial training and mitigating low efficiency, low generalization and unfairness, but remain to achieve poor performance against both strong white-box and black-box attacks, e.g., CW_∞ , Square and NATTACK, etc.

Recently, Bai et al. [11] and Yan et al. [12] investigated the adversarial robustness of DNNs from the perspective of channel-wise activations, which found that adversarial training can align the activation magnitudes of adversarial examples with those of their natural counterparts, but the over-activation of adversarial examples is still exist. To further improve the robustness of DNNs, Bai et al. [11] proposed Channel-wise Activation Suppressing (CAS) to suppress redundant activation of adversarial examples. Yan et al. [12] proposed Channel-wise Importance-based Feature Selection (CIFS) to suppress the channels that are negatively-relevant to predictions when processing adversarial examples. However, these methods also remain to achieve poor performance against both white-box attacks with weak transferability and black-box attacks.

To fill this gap, we propose a middle Feature layer Analysis and Conditional Matching prediction distribution (FACM) model to correct the output of DNN against adversarial samples with features extracted by the middle layers of DNN. The proposed FACM model consists of three modules: the middle feature layer analysis (FA) module, the conditional matching prediction distribution (CMPD) module and the output decision module, respectively. The FA module directly takes the output of the middle layers as the input to build the middle layer classifiers, and then the middle layer correction model can be constituted by the ensemble of the middle layer classifier and the DNN model. The CMPD module is used to build an autoencoder that is conditioned in the outputs of several middle layer classifiers, in order to reconstruct the input of the DNN with the objective of mitigating the effect of the perturbation. Particularly, the conditions involved in the

Corresponding author: Jie Lin.

Xiangyuan Yang, Jie Lin, Xinyu Yang and Peng Zhao are with School of Computer Science and Technology, Xi’an Jiaotong University, Xi’an, China (e-mail: ouyang_xy@stu.xjtu.edu.cn; {jielin, yxyphd, p.zhao}@mail.xjtu.edu.cn)

Hanlin Zhang is with Qingdao University, Qingdao, China (e-mail: hanlin@qdu.edu.cn)

autoencoder can improve the efficiency of reconstruction. In addition, the loss function of the autoencoder is generated by the Kullback-Leibler divergence between the predictions of the DNN on the original and reconstructed inputs. The output decision module can randomly select one or more correction models generated in both the FA and CMPD modules to correct the output through weighted fusion of these selected correction models. Because correction and diversity properties are introduced in FACM, the DNN's defense ability against both black-box attacks and white-box attacks with weak transferability can be improved. Our main contributions are summarized as:

- The correction property that the middle layers of the DNN can still extract the effective features of the original category of the adversarial sample is proposed and theoretically proved that can be used to correct the DNN's output.
- The middle Feature layer Analysis and Conditional Matching prediction distribution (FACM) model is proposed to correct the output of the DNN against adversarial samples with features extracted by middle layers of the DNN.
- The diversity property that the correction model in FACM is diverse against adversarial samples is proposed. The greater the attack strength, the more obvious the diversity.
- Extensive experiments are conducted to evaluate the effectiveness of our FACM model and FA model, and the evaluation results shown that our FACM model can efficiently improve the classification accuracy of the naturally trained DNN model against various attacks and FA model can efficiently improve the classification accuracy of the adversarially trained DNN model against white-box attacks with weak transferability and black-box attacks. Note that FA model includes the FA module and the output decision module, not the CMPD module.

II. PRELIMINARIES

In this section, the adversarial training, TRADES and matching prediction distribution, are mentioned briefly.

Standard Adversarial Training: Adversarial training is an effective defense method to train robust DNN models against adversarial attacks. With adversarial attacks as the data augmentation method, the model trained with adversarial examples achieves considerable robustness. Madry et al. [13] first formulate adversarial training as a min-max optimization problem:

$$\min_{f \in \mathcal{H}} \mathbb{E}_{(x,y) \sim \mathcal{D}} \left[\max_{\delta \in \mathcal{B}} L(f(x + \delta), y) \right] \quad (1)$$

where \mathcal{H} is the hypothesis space, \mathcal{D} is the distribution of the training dataset, L is a loss function, and \mathcal{B} is the allowed perturbation space that is usually selected as an L_p norm ball around x . The basic ideal of adversarial training is to find a perturbed image $x + \delta$ based on a given original image x , with the objective of maximizing the loss with respect to correct classification. Then, the model is trained by generated adversarial examples.

TRADES: To trade off natural and robust errors, Zhang et al. [10] trained a DNN model with both natural and adversarial data, and changed the min-max formulation as follows:

$$\min_{f \in \mathcal{H}} \mathbb{E}_{(x,y) \sim \mathcal{D}} \left[L(f(x), y) + \beta \cdot \max_{\delta \in \mathcal{B}} L_{KL}(f(x + \delta), f(x)) \right] \quad (2)$$

where L_{KL} is the Kullback-Leibler loss, β is a regularization parameter that controls the trade-off between standard accuracy and robustness. As shown in Eq. 2, when β increases, standard accuracy will decrease while robustness will increase, and vice versa.

Matching Prediction Distribution: To correct the output of the DNN against adversarial samples, Vacanti et al. [14] presents a novel adversarial correction model including an autoencoder that is trained with a custom loss function generated by the Kullback-Leibler divergence between the classifier predictions on the original and reconstructed instances:

$$\min_{\theta^\Phi, \theta^\Psi} \mathbb{E}_{(x,y) \sim \mathcal{D}} [L_{KL}(f(x), f(\Psi(\Phi(x))))] \quad (3)$$

where $\Phi(\cdot)$ and $\Psi(\cdot)$ are the encoder and decoder of autoencoder, respectively, θ^Φ and θ^Ψ are the weights of $\Phi(\cdot)$ and $\Psi(\cdot)$ that need to be optimized. This method is unsupervised, easy to train and does not require any knowledge about the underlying attack.

III. PROPOSED APPROACH

In this section, we present the FACM model, which consists of three modules: the middle feature layer analysis (FA) module, the conditional matching prediction distribution (CMPD) module and the output decision module. In this section, first the construction steps and the working principles of the FACM model is introduced, and then the working principle and theoretical analysis of FA, CMPD, output decision modules and FACM model are described in details.

A. Construction Steps and Working Principles of FACM Model

Construction Steps: Firstly, the middle layer correction model, denoted as $\{(f + f_i)(\cdot) | 1 \leq i \leq n - 1\}$, is constructed. Then, the conditional matching prediction distribution correction model, denoted as $\{g_i(\cdot) | 0 \leq i \leq n - 1\}$, is constructed. Finally, the output decision model, denoted as $h(\cdot)$, is constructed.

Working Principles: Taking an instance (x, y) as an example, firstly the weights vector $\omega = S(h(x))$ is calculated by the output decision model, where $S(\cdot)$ is the sigmoid function. Then, ω is normalized to $\bar{\omega}$. Thirdly, τ correction models are randomly extracted from all correction models (i.e. FACM, including the DNN model itself) according to probability vector $\bar{\omega}$. Finally, the average output of τ correction models is taken as the final prediction of the instance x .

B. Middle Feature Analysis Module

Definition 1: (Middle layer classifier) For an instance $(x, y) \sim \mathcal{D}$, the output of the i^{th} middle layer is denoted

as $l_i(x)$. The i^{th} middle layer classifier $f_i(\cdot)$ can be built by taking the output of the i^{th} middle layer $l_i(x)$ as the input:

$$\min_{\theta^i} \mathbb{E}_{(x,y) \sim \mathcal{D}} [L_{CE}(f_i(l_i(x)), y)] \quad (4)$$

where $L_{CE}(\cdot, \cdot)$ is the cross-entropy loss.

Definition 2: (Middle layer correction model) For the DNN $f(\cdot)$ and the i^{th} middle layer classifier $f_i(\cdot)$, the i^{th} middle layer correction model, denoted as $(f + f_i)(\cdot)$, can be constituted by the ensemble of $f(\cdot)$ and $f_i(\cdot)$.

In the middle layer correction model $(f + f_i)(\cdot)$, the middle layer classifier $f_i(\cdot)$ can correct the output of the DNN $f(\cdot)$ without any effect on the classification accuracy of $f(\cdot)$ on normal samples (i.e., the classification accuracy of $(f + f_i)(\cdot)$ is basically equal to that of $f(\cdot)$ on normal samples).

In the following, Definitions 3 and 4 are mentioned to define the classification sequence and corresponding classification sequence sub-space which are used in the proof of Proposition 1 to analyze the effectiveness of the middle layer correction model.

Definition 3: (Classification sequence) For an instance $(x, y) \sim \mathcal{D}$, the top i middle layer classifiers' classification sequence S_i can be denoted as $[\text{argmax}(f_1(x)), \text{argmax}(f_2(x)), \dots, \text{argmax}(f_i(x))]$.

Definition 4: (Classification sequence sub-space) In the input space \mathcal{D} of the DNN $f(\cdot)$, the sub-space $\mathcal{D}_i^{S_i}$ indicates that the sequence $[\text{argmax}(f_1(x)), \text{argmax}(f_2(x)), \dots, \text{argmax}(f_i(x))]$ is equal to S_i when $x \in \mathcal{D}_i^{S_i}$.

Proposition 1: The impact of adversarial examples on the middle layer is less than that on the last layer.

Proof 1: For any two adjacent middle layer classifiers f_i and f_{i+1} classified into the same correct category k , if the classification sequence of the top $i - 1$ middle layer classifiers is S_{i-1} , $\mathcal{D}_{i+1}^{[S_{i-1}, k, k]}$ is constrained in $\mathcal{D}_i^{[S_{i-1}, k]}$ (i.e., $\mathcal{D}_{i+1}^{[S_{i-1}, k, k]} \in \mathcal{D}_i^{[S_{i-1}, k]}$) and $\mathcal{D}_i^{[S_{i-1}, k]} - \mathcal{D}_{i+1}^{[S_{i-1}, k, k]}$ is classified into wrong categories other than k . The following two cases discuss that the correct classification of the classifiers $f_i(\hat{x})$ or $f_j(\hat{x}) (j < i)$ can make up for the wrong classification of the classifier $f_{i+1}(\hat{x})$ where \hat{x} is an adversarial examples, k is the original category:

- Case 1: $\hat{x} \notin \mathcal{D}_{i+1}^{[S_{i-1}, k, k]} \wedge \hat{x} \in (\mathcal{D}_i^{[S_{i-1}, k]} - \mathcal{D}_{i+1}^{[S_{i-1}, k, k]})$, where \hat{x} causes the classifier f_{i+1} to misclassify, while \hat{x} is still belong to $\mathcal{D}_i^{[S_{i-1}, k]}$ so that the classifier f_i can make the correct classification to \hat{x} .
- Case 2: $\exists j < i, \hat{x} \notin \mathcal{D}_{i+1}^{[S_{i-1}, k, k]} \wedge \hat{x} \notin (\mathcal{D}_i^{[S_{i-1}, k]} - \mathcal{D}_{i+1}^{[S_{i-1}, k, k]}) \wedge \hat{x} \in \mathcal{D}_j^{[S_{i-1}, [1 \dots j-1], k]}$, where \hat{x} causes the classifier $f_{j+1}, \dots, f_i, f_{i+1}$ to misclassify, while \hat{x} is still belong to $\mathcal{D}_j^{[S_{i-1}, [1 \dots j-1], k]}$ so that the classifier f_j can make the correct classification to \hat{x} , where $S_{i-1}[1 \dots j - 1]$ denotes the sub-sequence with indexes within $[1 \dots j - 1]$.

These two cases occur because the disturbance against the original normal sample is very small and as close to the original normal sample as possible in the definition domain. Therefore, adversarial samples only make the output layer of deep neural network output wrong classification, but have little

impact on the middle layer classifier (i.e., $f_i, i < n$, n is the depth of the DNN). Proof over.

However, a problem has arisen as follows: the middle layer classifier cannot completely make up for all adversarial samples because the outputs of the middle layer classifiers may not have the effective features of the original normal category. To solve the problem, a conditional matching prediction distribution module is proposed in Section III-C, which transforms the adversarial sample \hat{x} into \hat{x}' that can be classified correctly by the output layer of DNN.

C. Conditional Matching Prediction Distribution Module

The conditional matching prediction distribution (CMPD) correction model is actually an autoencoder, in which the input consists of a sample x and the concatenation of the outputs of several middle layer classifiers, and the output is a transformed sample x' . Note that, the different number of middle layers features as the conditions constructs the different CMPD correction model.

Definition 5: (The i^{th} CMPD correction model $g_i(\cdot)$) which emerges an encoder $\Phi(\cdot)$, a decoder $\Psi(\cdot)$ and the outputs of the top i middle layer classifiers as the conditions, i.e., $g_i(\cdot) = \Psi(\Phi(\cdot | f_1(\cdot), \dots, f_i(\cdot)) | f_1(\cdot), \dots, f_i(\cdot))$. The $g_i(\cdot)$ is built by:

$$\min_{g_i \in \mathcal{H}_{g_i}} \mathbb{E}_{(x,y) \sim \mathcal{D}} [L_{KL}(f(x), f(g_i(x)))] \quad (5)$$

where \mathcal{H}_{g_i} is the hypothesis space of g_i .

Definition 5 defines the composition and objective function of the i^{th} CMPD correction model. Note that, in our FACM model, because the dimensions of the input conditions are different, all the CMPD correction models share weights except for layers with conditional inputs in the encoder and decoder. When CMPD correction model g_0 does not have any conditional input, it can be considered as the MPD correction model $g(\cdot) = \Psi(\Phi(\cdot))$ (i.e., $g_0 = g$). Proposition 2 verify that the CMPD correction model is easier to converge than MPD correction model.

Proposition 2: For a learning task, in the case of conditional constraints, the less the mapping of learning, the less the complexity of the task, thereby leading to the faster and more stable convergence of the model training. With the conditions of given outputs of $f_1(\cdot), f_2(\cdot), \dots, f_i(\cdot)$, our CMPD correction model g_i simplifies the difficulty of the autoencoder learning task in comparison with MPD correction model g .

Proof 2: For the MPD correction model g , to correctly classify the sample x , the compound function $f \circ g(x)$ needs to find a classification sequence $[\text{argmax}(f_1 \circ g(x)), \text{argmax}(f_2 \circ g(x)), \dots, \text{argmax}(f_n \circ g(x))]$ from m^n classification sequences where m is the number of categories and n is the layer depth of the DNN. While, for the CMPD correction model g_i , to correctly classify the sample x , because the classification sequence S_i is the known conditions, the compound function $f \circ g_i(x)$ only needs to find a classification sub-sequence $[S_i, \text{argmax}(f_{i+1}(g_i(x))), \dots, \text{argmax}(f_n(g_i(x)))]$ from m^{n-i} classification sequences. According to the concept of the hypothesis space and growth function in computational learning theory [15], the growth functions of the hypothesis space of g and g_i are calculated as Eq. 6, where the hypothesis

space is the set of all possible mappings and the growth function represents the maximum number of possible results that M samples are labeled in the hypothesis space.

$$\begin{cases} \Pi_{\mathcal{H}_g}(M) = M^{m^n} \\ \Pi_{\mathcal{H}_{g_i}}(M) = M^{m^{n-i}} \end{cases} \quad (6)$$

where \mathcal{H}_g and \mathcal{H}_{g_i} denote hypothesis space of the MPD correction model g and the CMPD correction model g_i respectively, $\Pi_{\mathcal{H}_g}$ and $\Pi_{\mathcal{H}_{g_i}}$ denote the growth function of \mathcal{H}_g and \mathcal{H}_{g_i} respectively, M is the size of train dataset. Due to $\Pi_{\mathcal{H}_g}(M) \gg \Pi_{\mathcal{H}_{g_i}}(M)$, the CMPD correction model converges faster than the MPD correction model.

According to Theorem 12.2 [15], for any M , $0 < v < 1$, $g \in \mathcal{H}_g$ and $g_i \in \mathcal{H}_{g_i}$, we have

$$\begin{cases} P(|E(g) - \hat{E}(g)| > v) \leq 4\Pi_{\mathcal{H}_g}(2M) \exp(-\frac{Mv^2}{8}) \\ P(|E(g_i) - \hat{E}(g_i)| > v) \leq 4\Pi_{\mathcal{H}_{g_i}}(2M) \exp(-\frac{Mv^2}{8}) \end{cases} \quad (7)$$

where $P(|E(g) - \hat{E}(g)| > v)$ and $P(|E(g_i) - \hat{E}(g_i)| > v)$ respectively denote the probabilities of the MPD correction model g and the CMPD correction model g_i which do not converge to the expectation error v . Due to $4\Pi_{\mathcal{H}_{g_i}}(2M) \exp(-\frac{Mv^2}{8}) \ll 4\Pi_{\mathcal{H}_g}(2M) \exp(-\frac{Mv^2}{8})$, the possible values and ranges of $P(|E(g_i) - \hat{E}(g_i)| > v)$ are smaller, i.e., g_i has a smaller probability of non convergence. Therefore, the CMPD correction model converges more stable than the MPD correction model. Proof over.

When $i \geq \arg \max_j (\arg \max f_j(x) \neq \arg \max f_j(\hat{x}))$, the CMPD correction model g_i cannot be used to transfer the adversarial sample \hat{x} because the classification sequence of the conditions hardly changes, i.e., the sequence $[\arg \max(f_1 \circ g_i(x)), \arg \max(f_2 \circ g_i(x)), \dots, \arg \max(f_i \circ g_i(x))]$ hardly recovers to the original sequence $[\arg \max(f_1(x)), \arg \max(f_2(x)), \dots, \arg \max(f_i(x))]$. Meanwhile, according to two cases analysis in the proof of Proposition 1, different adversarial samples need different middle layer correction models. Hence, output decision model in Section III-D calculate the weights of each correction model in the FA and CMPD modules for each adversarial sample, then select the correction model with the weights.

D. Output Decision Module

Because the adversarial samples will make the deep neural network take an unusual activation path [16], the outputs of all middle layer classifier can be used to decide whether use the correction model or not and determine the weight of each correction model. Therefore, for a sample (x, y) , the training data of output decision model $h(\cdot)$ can be defined as $X^h(x)$ and $Y^h(x)$, which are the input and output annotation function of h , respectively. $X^h(x)$ indicates the concatenation of all middle layer classifiers' output. $Y^h(x)$ represents a 0-1 vector indicating whether the DNN or each correction model (i.e., each element in $[f(x), (f + f_1)(x), \dots, (f + f_{n-1})(x), f \circ g_0(x), \dots, f \circ g_{n-1}(x)]$) is classified correctly or not. Algorithm 1 indicates the training of output decision model where $F(\cdot)$ is the ensemble model of all correction models and the

Algorithm 1 (Output Decision model training): PGD adversarial training for T epochs, given some radius set \mathcal{E} , adversarial step size \mathcal{A} , N PGD steps and a dataset of size M , robust output decision model h and its weights θ_h .

```

 $\mathcal{D} = \{x_i | i \leq M\}$ 
for  $\epsilon, \alpha$  in  $\mathcal{E}, \mathcal{A}$  do
  for  $i = 1$  to  $M$  do
    //Perform PGD adversarial attack
     $\delta = 0$  //or randomly initialized
    for  $j = 1$  to  $N$  do
       $\delta = \delta + \alpha \cdot \text{sign}(\nabla_{\delta} L_{CE}(F(x_i + \delta), y_i))$ 
       $\delta = \max(\min(\delta, \epsilon), -\epsilon)$ 
    end for
     $\mathcal{D} = \mathcal{D} \cup \{x_i + \delta\}$ 
  end for
end for
for  $t = 1$  to  $T$  do
  for  $x$  in  $\mathcal{D}$  do
    // Update model weights
     $\theta_h = \theta_h - \nabla_{\theta_h} L_{MFL}(x)$ 
  end for
end for

```

DNN model. Because the accuracies of different correction models are different on adversarial samples, for the output decision model h , the amount of training data of different labels is unbalanced. Hence, the multi-label focal loss is used as the loss function, which is defined as:

$$L_{MFL}(x) = \sum_i -Y^h(x)_i \cdot (1 - S(h(X^h(x)))_i)^\gamma \cdot \log(S(h(X^h(x)))_i) \quad (8)$$

where $S(\cdot)$ is the sigmoid function, γ is an adjustable factor, $S(h(X^h(x)))_i$ and $Y^h(x)_i$ are the i^{th} element in these vectors, respectively.

E. FACM Model

Besides the correction property introduced in Sections III-B and III-C, the diversity property of FACM is introduced in Proposition 3.

Proposition 3: The correction model in FACM is diverse against adversarial samples. The greater the attack strength, the more the obvious the diversity.

Proof 3: Due to the complementarity of FA module and CMPD module in FACM, we discuss the diversity of the correction models in FA and CMPD, respectively.

In FA, Figs. 5, 6, 7 and 8 show that there are differences between the correction models against adversarial samples on the naturally trained DNN model and the adversarially trained DNN model for MNIST, CIFAR10/100 datasets, and the greater the attack strength, the more the obvious the differences. Hence, the diversity property of FA is correct with high confidence.

In CMPD, Figs. 9, 10, 11 and 12 also prove the diversity property of CMPD with high confidence. Proof over.

Based on Proposition 3, due to the diversity of the correction models in FACM and the randomness of the output decision

module, FACM can significantly improve the robustness of DNN against white-box attacks with weak transferability and black-box attacks. Two reasons briefly explain why the combination of diversity and randomness can defend white-box attacks with weak transferability and black-box attacks. (i) Because the attacked DNN model (i.e., the DNN f or the ensemble correction models) is not equal to the random selected correction model (i.e., the prediction model), the white-box attack on FACM model is not the real white-box attack, but almost the black-box transfer attack. Therefore, the performance of white-box attacks on FACM is decreased, especially white-box attacks with weak transferability [17]. The diversity of the correction models in FACM further decreases the performance of white-box attacks with weak transferability. (ii) The existence of diversity and randomness will lead to inaccurate gradient estimation and model optimization of black-box attacks.

IV. EXPERIMENTS AND RESULTS

In this section, the experiment is conducted to validate the effectiveness of the proposed model (FACM and FA) on achieving the robust output of the DNN model.

A. Experimental Setting

Our experiments are conducted on benchmark adversarial learning datasets, including MNIST [18], CIFAR10 [19] and CIFAR100 [19] datasets. For MNIST dataset, the algorithms with the model architecture MNISTNet [20] are evaluated, where MNISTNet includes 4 convolutional layers and 3 fully connected layers. For both CIFAR10 and CIFAR100 datasets, the algorithms with the model architecture WRN-16-4 [21] are evaluated, where WRN-16-4 includes 4 basic blocks. The architecture of middle layer classifier is a fully connected layer, in which the input is the output of middle layer and the output is the probability vector of each category. The auto-encoder architecture of the CMPD module is similar across the datasets and consists of 3 convolutional layers in both the encoder and the decoder. As baselines, 7 adversarial training methods are chosen, i.e., Fast Adversarial Training (Fast-AT) [5], You Only Propagate Once (YOPO) [8], Adversarial Training with Hypersphere Embedding (ATHE) [4], Fair Robust Learning (FRL) [9], Friendly Adversarial Training (FAT) [6], TRADES [10] and Adversarial Training with Transferable Adversarial examples (ATTA) [7], and 2 channel-wise activation suppressing methods, i.e., Channel-wise Activation Suppressing (CAS) [11] and Channel-wise Importance-based Feature Selection (CIFS) [12]. Note that the middle layer can be a single layer or a network block.

In our implementation for FACM model, during the training process, we firstly train the DNN model using natural training or TRADES adversarial training, then the FA module and the CMPD module are trained by stochastic gradient descent (SGD) optimizer with learning rate as 0.0005 and 0.001 for 10 and 30 epochs, respectively. Finally, the output decision module is trained by the SGD optimizer with learning rate as 0.1 for 20 epochs. Note that, in order to avoid overfitting, the CMPD module for the MNISTNet is trained for

5 epochs. Multistep learning rate scheduler is used in every training phase in FACM, and we decay the learning rate by 0.1 at the 1/4 and 3/4 of the total epochs. During the evaluation phase, we report each trained model's classification accuracy, model build time, attack time and inference time on clean samples, 4 white-box attacks with good transferability, (i.e., Fast Gradient Sign Method (FGSM) [22], Projected Gradient Descent (PGD) [23], Momentum Iterative FGSM (MIFGSM) [24], AutoAttack [25]), 3 white-box attacks with weak transferability (i.e., Carlini Wagner L_∞ and L_2 (CW_∞ and CW_2) [2] and DeepFool L_2 [3]) and 2 black-box attacks (Square [26] and NATTACK [27]). All test samples in MNIST, CIFAR10 and CIFAR100 are used to evaluate the accuracy of model with the white-box attacks. For black-box attacks, the first 1000 samples in the test samples are used for evaluation with the Square attack, and the first 200 samples for evaluation with the NATTACK attack. Note that the attack time and inference time are the total calculation time on the test set, not the average calculation time. The **average** or **avg.** in Tables I, II, III, IV, V and VI is the average classification accuracy on the white-box attacks with weak transferability and the black-box attacks.

The aforementioned white-box attacks and black-box attacks are implemented in [28]. The hyperparameters of each attack are introduced as follows. The attack strength ϵ is set to 8/255 on CIFAR10/100 and 0.3 on MNIST for FGSM, PGD, MIFGSM, AA, CW_∞ and NATTACK, and 0.05 on CIFAR10/100 and 0.3 on MNIST for Square. The step size α is set to 0.8/255 on CIFAR10/100 and 0.03 on MNIST for PGD, and 2/255 on CIFAR10/100 and 0.1 on MNIST for MIFGSM. The number of steps is set to 20 on CIFAR10/100 and 40 on MNIST for PGD, 10 on CIFAR10/100 and 50 on MNIST for CW_2 and CW_∞ , 5 on all datasets for MIFGSM, 50 on all datasets for DeepFool L_2 , 5000 on all datasets for Square and 500 on all datasets for NATTACK. The learning rate is set to 0.2 on CIFAR10/100 and 1.0 on MNIST for CW_2 , and 0.01 on all datasets for CW_∞ . The overshoot is 0.02 on all datasets for DeepFool L_2 . The population is 100 on all datasets for NATTACK. The box-constraint is 0.005 on CIFAR10/100 and 10 on MNIST for CW_2 . In addition, the hyperparameters of all the baselines are set to the optimal parameters in their original papers.

To explain the diversity of the correction model in FACM against adversarial samples, a difference metric $\xi(\rho_1, \rho_2, \mathcal{S})$ between two correction models ρ_1 and ρ_2 on test set \mathcal{S} is introduced as follows:

$$\xi(\rho_1, \rho_2, \mathcal{S}) = \frac{\|\mathbf{v}_S^{\rho_1} | \mathbf{v}_S^{\rho_2}\|_1 - \|\mathbf{v}_S^{\rho_1} \& \mathbf{v}_S^{\rho_2}\|_1}{\|\mathbf{v}_S^{\rho_1} | \mathbf{v}_S^{\rho_2}\|} \quad (9)$$

where ρ_1, ρ_2 are two correction models, \mathcal{S} is the test set, $\mathbf{v}_S^{\rho_1}$ denotes 0-1 vector in which each element represents whether the correction model ρ_1 correctly predicts a test sample in \mathcal{S} , $|$ and $\&$ represent OR and AND, respectively, $\|\cdot\|_1$ denotes the 1 norm. Note that, the CMPD model should be combined with the DNN model f for correction, i.e., $f \circ g_i$.

We consider two settings on the attacks: grey-box and white-box. **The grey-box attacks of FACM** (FACM-grey) have full knowledge of the DNN model but not the defense model

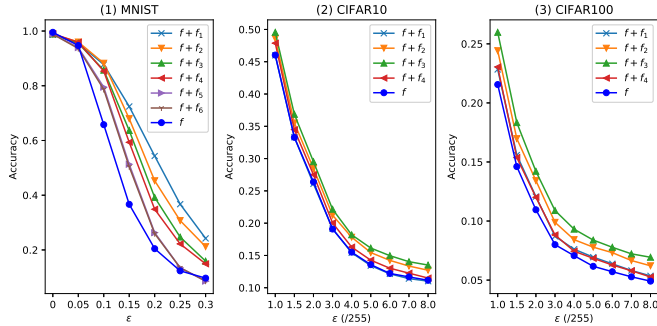


Fig. 1. The test accuracy curves of different middle layer classifiers $\{f + f_i\}$ and the DNN model f on MNIST, CIFAR10 and CIFAR100 when the naturally trained DNN model f (i.e., FACM-grey) is attacked by FGSM with different ϵ .

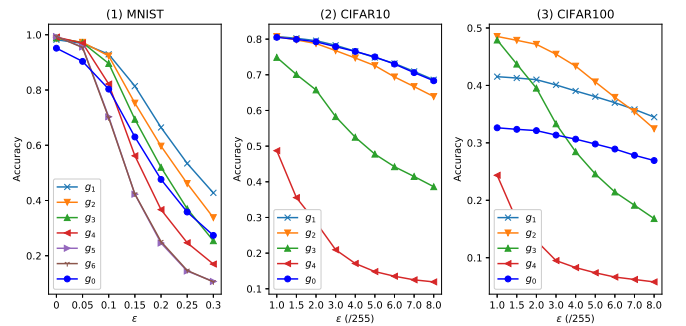


Fig. 2. The test accuracy curves of different CMPD models $\{g_i\}$ (including matching prediction distribution model g_0) on MNIST, CIFAR10 and CIFAR100 when the naturally trained DNN model f (i.e., FACM-grey) is attacked by FGSM with different ϵ .

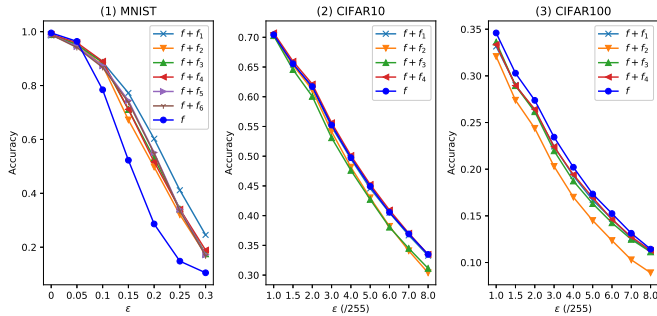


Fig. 3. The test accuracy curves of different middle layer classifiers $\{f + f_i\}$ and the DNN model f on MNIST, CIFAR10 and CIFAR100 when the ensemble model of the naturally trained DNN model f and the middle layer classifiers $\{f + f_i\}$ and the CMPD models $\{g_i\}$ (i.e., FACM-white) is attacked by FGSM with different ϵ .

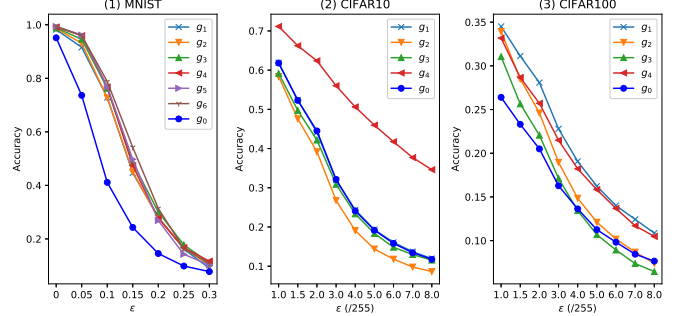


Fig. 4. The test accuracy curves of different CMPD models $\{g_i\}$ (including matching prediction distribution model g_0) on MNIST, CIFAR10 and CIFAR100 when the ensemble model of the naturally trained DNN model f and the middle layer classifiers $\{f + f_i\}$ and the CMPD models $\{g_i\}$ (i.e., FACM-white) is attacked by FGSM with different ϵ .

of the FA module, the CMPD module and output decision module. **The white-box attacks of FACM (FACM-white)** not only have the full knowledge of the DNN model, but also the defense model about FACM. All experiments are run on single machine with four GeForce RTX 2080tis using Pytorch.

B. Correction Effect of Middle Layers Features

To verify that the middle layers features can correct the output of the DNN f when f is attacked (i.e., FACM-grey), we compared the test accuracy of f with the middle layer correction models $f + f_i$ on MNIST, CIFAR10 and CIFAR100 under FGSM with different attack strength ϵ . As shown in Fig. 1, the blue curve represents the test accuracy of f varies with the attack strength ϵ and the other curves represent the middle layer correction models $\{f + f_i\}$. The results show that the test accuracies of all the middle layer correction models $\{f + f_i\}$ are higher than the DNN model f on all datasets with all attack strengths. In addition, Fig. 5 verifies the diversity property of FA when f is attacked (i.e., FACM-grey). As shown in Fig. 5, the difference matrix heatmaps on different datasets with different attack strengths show that: as the attack strength gradually increases, the differences between the correction models become more and more significant.

Fig. 3 shows that the test accuracies of all the middle layer correction models $\{f + f_i\}$ are higher than the DNN model f on MNIST with various attack strengths, less or equal to the

DNN model f on CIFAR10 and CIFAR100 with any attack strength when FACM-white is attacked by FGSM. Therefore, the correction property of FA is effective on MNIST, but ineffective on CIFAR10/100 when FACM-white is attacked by FGSM. In addition, Fig. 7 verifies the diversity property of FA when FACM-white is attacked by FGSM. As shown in Fig. 7, the difference matrix heatmaps on different datasets under different attack strengths show that: as the attack strength gradually increases, the differences between the correction models become more and more significant.

To further verifies the diversity property of FA on the adversarially trained DNN model, Figs. 6 and 8 represent the difference matrix heatmaps of the middle layer correction models on the TRADES trained DNN when FACM-grey and FACM-white are attacked by FGSM, respectively. As the attack strength gradually increases, the differences between the middle layer correction models become larger but not significant because the size of the common correction samples set is large (the test accuracy of the middle layer correction models in the TRADES trained DNN is higher than the naturally trained DNN under the FGSM attack) so that the difference calculated by Eq. 9 has slight increased.

C. Comparison between CMPD and MPD

To verify the effectiveness of the CMPD correction models when the DNN model f is attacked (i.e., FACM-grey), we

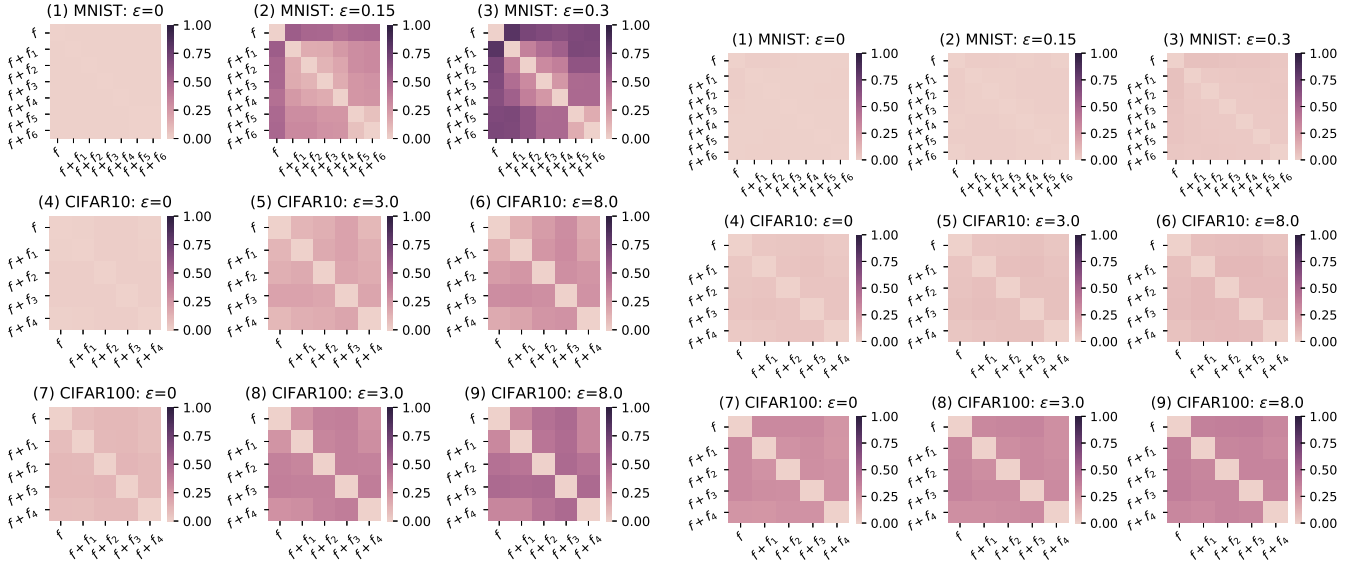


Fig. 5. The difference (which is calculated by Eq. 9) matrix heatmap between different middle layer classifiers $\{f + f_i\}$ and the DNN model f on MNIST, CIFAR10 and CIFAR100 when the naturally trained DNN model f (i.e., FACS-Grey) is attacked by FGSM with different ϵ (/255 on CIFAR10/100).

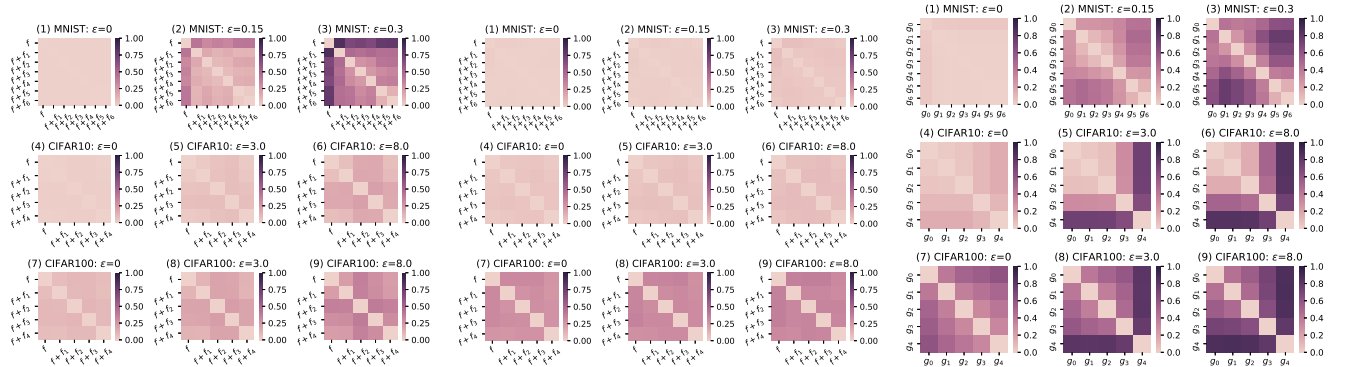


Fig. 7. The difference (which is calculated by Eq. 9) matrix heatmap between different middle layer classifiers $\{f + f_i\}$ and the DNN model f on MNIST, CIFAR10 and CIFAR100 when the naturally trained DNN model f (i.e., FACS-Grey) is attacked by FGSM with different ϵ (/255 on CIFAR10/100).

compared the test accuracies of the CMPD correction models $\{g_i\}$ with the MPD correction model g_0 on MNIST, CIFAR10 and CIFAR100 under FGSM with different attack strength ϵ . As shown in Fig. 2, the blue curve represents the test accuracy of g_0 and the other curves represent $\{g_i\}$. Fig. 2(1),(3) show that the test accuracy of the CMPD correction model g_i using the outputs of the shallow middle layer classifiers (i.e., i is small) as a condition is higher than that of the MPD correction model g_0 on MNIST and CIFAR100 datasets. Fig. 2(2) shows that the CMPD correction model g_i using the output of the shallow middle layer classifiers as a condition has comparable performance to the MPD correction model g_0 . In addition, Fig. 9 verifies the diversity property of the CMPD correction model when FACS-Grey is attacked by FGSM. As

shown in Fig. 9, the difference matrix heatmaps on different datasets under different attack strengths show that: as the attack strength gradually increases, the differences between the CMPD correction models become more and more significant.

When FACS-white is attacked by FGSM, Fig. 4(1),(3) show that the test accuracies of all CMPD correction models $\{g_i\}$ are higher than that of the MPD correction model g_0 on MNIST and CIFAR100, and Fig. 4(2) shows that the majority of the CMPD correction models $\{g_i\}$ have comparable performance to the MPD correction model g_0 . Therefore, the correction property of CMPD is effective on MNIST and CIFAR100. In addition, Fig. 11 verifies the diversity property of the CMPD correction model when FACS-white is attacked by FGSM. As shown in Fig. 11, the difference

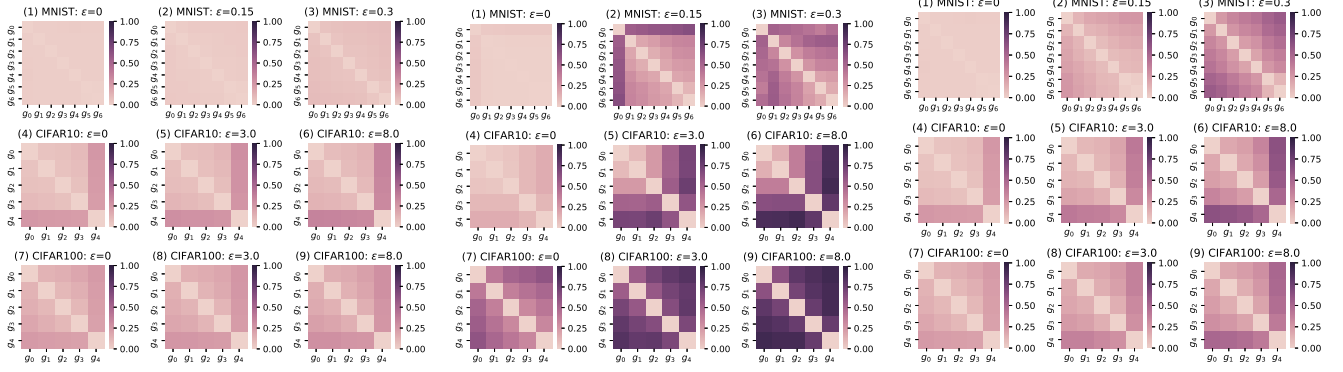


Fig. 10. The difference (which is calculated by Fig. 11. The difference (which is calculated by Fig. 12. The difference (which is calculated by Eq. 9) matrix heatmap between different CMPD Eq. 9) matrix heatmap between different CMPD Eq. 9) matrix heatmap between different CMPD models $\{g_i\}$ on MNIST, CIFAR10 and CIFAR100 models $\{g_i\}$ on MNIST, CIFAR10 and CIFAR100 models $\{g_i\}$ on MNIST, CIFAR10 and CIFAR100 when the TRADES trained DNN model f (i.e., when the ensemble model of the naturally trained when the ensemble model of the TRADES trained FACM-grey) is attacked by FGSM with different ϵ DNN model f and the middle layer classifier $f+f_i$ DNN model f and the middle layer classifier and the CMPD models $\{g_i\}$ (i.e., FACM-white) $\{f+f_i\}$ and the CMPD models $\{g_i\}$ (i.e., FACM- is attacked by FGSM with different ϵ (/255 on CIFAR10/100). is attacked by FGSM with different ϵ (/255 on white) is attacked by FGSM with different ϵ (/255 on CIFAR10/100).

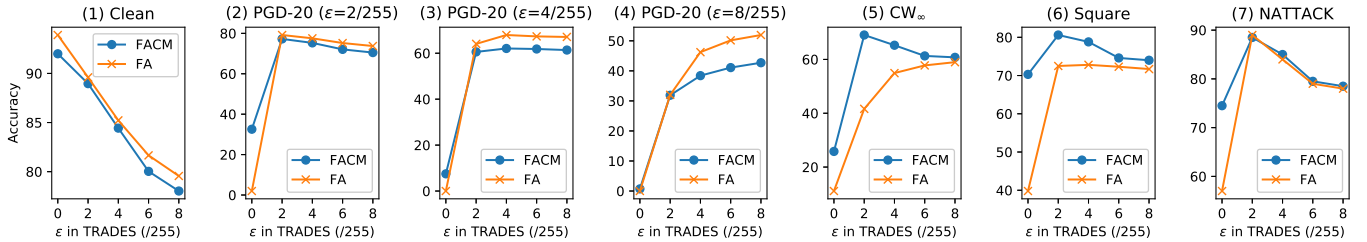


Fig. 13. The effect of different ϵ in TRADES adversarial training on the CIFAR10 test accuracy(%) of FACM model and FA model on various attack types under FACM-white and FA-white.

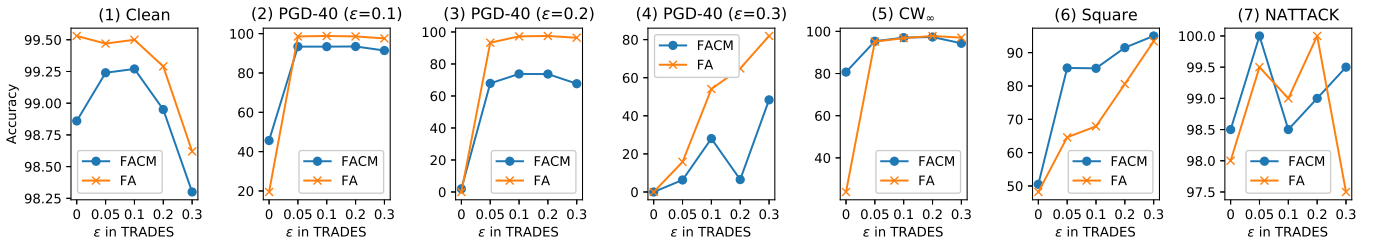


Fig. 14. The effect of different ϵ in TRADES adversarial training on the MNIST test accuracy(%) of FACM model and FA model on various attack types under FACM-white and FA-white.

matrix heatmaps on different datasets with different attack strengths show that: as the attack strength gradually increases, the difference between the CMPD correction models become more significant.

To further verifies the diversity property of the CMPD correction model on the adversarially trained DNN model, Figs. 10 and 12 represent the difference matrix heatmaps of the CMPD correction models in the TRADES trained DNN when FACM-grey and FACM-white are attacked by FGSM, respectively. As the attack strength gradually increases, the differences between the CMPD correction models become larger but not significant because the test accuracy of the CMPD correction models built in the TRADES trained DNN is higher than that in the naturally trained DNN under the FGSM attack, so that the size of the common correction samples

set is large and the difference calculated by Eq. 9 has slight increased.

D. Comparison between FACM and FA

Fig. 13 evaluate the effect of TRADES trained model with different ϵ on FA and FACM for CIFAR10 under different types of attacks, and Fig. 14 for MNIST. As shown in Figs. 13 and 14, when ϵ is equal to 0, the TRADES ($\epsilon = 0$) trained model (i.e., the naturally trained DNN model) with FACM is better than FA against all types of attacks. However, when ϵ is greater than 0, the TRADES trained model with FA is better than FACM for a majority of white-box attacks. As ϵ in TRADES increases, the test accuracy of FA gradually approaches FACM against CW_∞ and all black-box attacks. In conclusion, combining the aforementioned statements, the

TABLE I

EVALUATIONS (TEST ACCURACY(%)) OF THE NATURALLY TRAINED DNN MODEL WITH OR WITHOUT FACM ON CIFAR10/100 AND MNIST DATASETS. F1, P1, SQ, NA AND DF_2 REPRESENT FGSM($\epsilon=2/255$ ON CIFAR10/100 AND $\epsilon=0.1$ ON MNIST), PGD(ϵ, α , STEP NUMBER= $2/255, 0.2/255, 20$ ON CIFAR10/100 AND ϵ, α , STEP NUMBER= $0.1, 0.01, 40$ ON MNIST), SQUARE, NATTACK AND DEEPFOOL L_2 , RESPECTIVELY. NOTE THAT THE ATTACK STRENGTH OF SQUARE IS 0.05 ON CIFAR10/100 RATHER THAN 0.031.

Method		Clean	White-box attacks with							Black-box attacks		Avg.
			good transferability				weak transferability			Sq	NA	
			F1	FGSM	P1	PGD	DF_2	CW_2	CW_∞			
CIFAR 10	Natural	94.41	24.86	9.69	1.28	0	3.96	9.59	0	0	1.5	3.01
	FACM-white($\tau=3$)	91.86	60.26	26	32.86	0.66	12.24	17.71	23.37	70.1	80.5	40.78
	FACM-grey($\tau=3$)	92.09	49.61	48.43	25.93	10.67	79.7	29.51	51.87			62.34
CIFAR 100	Natural	75.84	11.08	5.3	0.6	0	5.99	4.06	0	0	0	2.01
	FACM-white($\tau=3$)	73.44	28.78	10.64	10.22	0.32	40.92	10.29	20.73	34.3	49.5	31.15
	FACM-gray($\tau=3$)	72.94	26.07	24.06	11.6	19.71	55.62	12.76	35.71			37.58
MNIST	Natural	99.53	65.78	9.7	19.48	0	46.13	2.7	0	0	32	16.17
	FACM-white ($\tau=1$)	98.61	78.91	13.71	47.08	0	16.32	77.94	47.53	61.8	99	60.52
	FACM-grey ($\tau=1$)	98.68	82.91	22.45	59.49	8.08	86.37	47.62	72.09			73.38

TABLE II

EVALUATIONS (TEST ACCURACY(%)) OF THE ADVERSARIALLY TRAINED DNN MODEL WITH OR WITHOUT FA ON CIFAR10/100 AND MNIST DATASETS. MI, AA, SQ, DF_2 AND NA REPRESENT MIFGSM, AUTOATTACK, SQUARE, DEEPFOOL L_2 AND NATTACK, RESPECTIVELY. NOTE THAT THE ATTACK STRENGTH OF SQUARE IS 0.05 ON CIFAR10/100 RATHER THAN 0.031.

Method		Clean	White-box attacks with							Black-box attacks		Avg.
			good transferability				weak transferability			Sq	NA	
			FGSM	PGD	MI	AA	DF_2	CW_2	CW_∞			
CIFAR 10	TRADES [10]	80.98	55.8	51.83	53.76	47.2	0.59	25.2	48.54	34.4	69	35.55
	FA-white($\tau=1$)+TRADES	79.42	55.09	51.63	53.66	47.1	33.66	27.96	61.78	72.6	76	54.4
	FA-grey($\tau=1$)+TRADES	79.47	55.59	51.86	53.99	-	35.42	27.69	59.1			54.16
CIFAR 100	TRADES [10]	55.91	29.23	26.91	27.82	21.7	0.36	8.9	22.36	13.3	39.5	16.88
	FA-white($\tau=3$)+TRADES	51.17	27.62	26.33	26.83	22.0	25.46	12.67	36.53	46.7	51	32.17
	FA-grey($\tau=3$)+TRADES	51.34	28.81	27.11	27.91	-	32.99	13.99	38.17			36.57
MNIST	TRADES [10]	99.48	93.36	70.69	82.32	27.7	4.43	68.17	96.19	19.7	95.5	56.80
	FA-white($\tau=2$)+TRADES	98.62	91.09	81.93	83.68	52.9	40.79	96.37	97.03	93.4	97.5	85.02
	FA-grey($\tau=2$)+TRADES	98.69	94.11	83.8	88.21	-	66.6	85.99	97.45			88.19

TABLE III

EVALUATIONS (TEST ACCURACY(%)) OF DIFFERENT ADVERSARIAL TRAINING METHODS ON CIFAR10 USING WHITE-BOX ATTACKS WITH WEAK TRANSFERABILITY AND BLACK-BOX ATTACKS. DF_2 REPRESENTS DEEPFOOL L_2 .

Method	White-box attacks with weak transferability			Black-box attacks			Average
	DF_2	CW_2	CW_∞	Square ($\epsilon=0.031$)	Square ($\epsilon=0.05$)	NATTACK	
Fast-AT [5]	0.71	21.3	45.03	49.0	26.3	68.5	35.14
YOPO-5-3 [8]	2.13	11.73	33.59	38.9	17.7	60	27.34
ATHE [4]	0.42	24.13	48.13	52.6	33.8	69.5	38.10
FRL [9]	1.82	5.4	21.44	26.3	9.3	50.5	19.13
FAT [6]	0.48	25.13	48.11	51.7	32	69	37.74
ATA [7]	0.58	21.78	44.97	46.8	30.9	64	34.84
FA-white($\tau=1$)+TRADES	33.66	27.96	61.78	76.2	72.6	76	58.03

naturally trained DNN model with FACM is better than FA. On the contrary, the TRADES trained model with FA is better than FACM. Therefore, in the following experiments, FACM is used for the naturally trained DNN model and FA is used for the adversarially trained DNN model.

E. Effect of FACM on the Naturally Trained DNN Model

To verify that FACM can effectively improve the robustness of naturally trained DNN model against various attacks, especially white-box attacks with weak transferability and black-box attacks, under the slight decrease of performance on clean samples, we compare the classification accuracy of the naturally trained DNN model with and without FACM

on CIFAR10/100 and MNIST. As shown in Table I, for the setting of FACM-white, FACM can improve the classification accuracy against white-box attacks with good transferability, and the smaller the attack strength ϵ in white-box attacks with good transferability is, the more obvious the increase of classification accuracy on each datasets. FACM can significantly improve the classification accuracy against white-box attacks with weak transferability and black-box attacks, specifically, the average improvement is 37.77% on CIFAR10, 29.14% on CIFAR100 and 44.35% on MNIST. The classification accuracy of clean samples decreases by 1.56%, 4.74% and 0.86% on CIFAR10/100 and MNIST, respectively. For the setting of FACM-grey, the classification accuracy against clean samples

TABLE IV
EVALUATIONS (TEST ACCURACY(%)) OF DIFFERENT ADVERSARIAL TRAINING METHODS ON CIFAR100 USING WHITE-BOX ATTACKS WITH WEAK TRANSFERABILITY AND BLACK-BOX ATTACKS. DF_2 REPRESENTS DEEPFOOL L_2

Method	White-box attacks with weak transferability			Black-box attacks			Average
	DF_2	CW_2	CW_∞	Square ($\epsilon=0.031$)	Square ($\epsilon=0.05$)	NATTACK	
Fast-AT [5]	2.49	17.78	0	0	0	0	3.38
YOPO-5-3 [8]	0.82	6.86	20.83	23.5	11	36	16.5
ATHE [4]	0.43	10.99	24.82	26.8	14.8	38.5	19.39
FRL [9]	1.93	2.67	6.94	8.1	2.8	19	6.91
FAT [6]	0.57	9.03	22.43	23.6	13.8	36	17.57
ATTA [7]	0.63	8.17	13.98	13.9	9.7	20	11.06
FA-white($\tau=3$)+TRADES	25.46	12.67	36.53	50.6	46.7	51	37.16

TABLE V
EVALUATIONS (TEST ACCURACY(%)) OF DIFFERENT ADVERSARIAL TRAINING METHODS ON MNIST USING WHITE-BOX ATTACKS WITH WEAK TRANSFERABILITY AND BLACK-BOX ATTACKS. DF_2 REPRESENTS DEEPFOOL L_2

Method	White-box attacks with weak transferability			Black-box attacks			Average
	DF_2	CW_2	CW_∞	Square ($\epsilon=0.3$)	Square ($\epsilon=0.4$)	NATTACK	
Fast-AT [5]	67.16	51.21	90.61	70.3	0	95.5	62.43
YOPO-5-10 [8]	33.82	46.36	85.66	69.6	5.3	90	55.12
ATHE [4]	1.77	95.23	95.76	86.2	0	97	62.66
FRL [9]	16.8	73.11	93.8	67.2	0	94.5	57.57
FAT [6]	0.79	76.06	95.67	59.3	0	96	54.64
ATTA [7]	2.5	89.27	96.81	92.4	0	97	63.00
FA-white($\tau=2$)+TRADES	40.79	96.37	97.03	93.4	27.9	97.5	75.50

TABLE VI
EVALUATIONS (TEST ACCURACY(%)) OF DIFFERENT CHANNEL-WISE ACTIVATION SUPPRESSING METHODS ON CIFAR10 USING VARIOUS ATTACKS. CL, F, P, MI, AA, DF_2 , SQ AND NA REPRESENT CLEAN, FGSM, PGD, MIFGSM, AUTOATTACK, DEEPFOOL L_2 , SQUARE AND NATTACK.

Method	Cl	White-box attacks with								Black-box attacks		Avg.
		good transferability				weak transferability				attacks		
		F	P	MI	AA	DF_2	CW_2	CW_∞	Sq	NA		
WRN-16-4	CAS+TRADES [11]	80.92	51.36	46.92	49.22	42.7	0.48	20.4	44.44	65.2	80	42.10
	Our FA-white($\tau=1$)+TRADES	79.42	55.09	51.63	53.66	47.1	33.66	27.96	61.78	72.6	76	54.4
ResNet18	CIFS [12]	82.46	61.07	54.66	58.02	-	0.66	37.99	53.74	39.8	66.5	39.74
	Our FA-white($\tau=3$)+CIFS	82.20	59.48	53.98	56.51	-	9.59	37.43	63.48	73.4	78	52.38

TABLE VII
THE BUILD TIME (MINS) OF DIFFERENT METHODS FOR BUILDING ROBUST MODELS ON MNIST AND CIFAR10/100.

	Natural Train	Fast-AT	YOPO	ATHE	FRL	FAT	ATTA	TRADES	Our FACM	Our FACM+TRADES
MNIST	8.5	13.6	43.3	122.6	39.9	161.8	63.6	93.1	163.2	213.7
CIFAR10	50.7	61.4	134.8	601.5	708.1	507.9	183.6	280.7	236.6	687.4
CIFAR100	114.8	45.6	66.3	558.2	1485	1015	165.2	498.5	235.8	687.2

and various attacks is higher than that of FACM-white.

F. Effect of FA on the Adversarially Trained DNN Model

To verify that FA can effectively improve the robustness of adversarially trained DNN model against white-box attacks with weak transferability and black-box attacks, under the usually slight decrease of performance against clean samples and white-box attacks with good transferability, we compare the classification accuracy of the TRADES trained model with and without FA on CIFAR10/100 and MNIST. As shown in Table II, for the setting of FA-white, FA can significantly improve the classification accuracy against white-box attacks with weak transferability and black-box attacks, specifically,

the average improvement is 18.85% on CIFAR10, 15.29% on CIFAR100 and 28.22% on MNIST. The average classification accuracy against clean samples and white-box attacks with good transferability decreases by 0.53%, 1.52% on CIFAR10/100, respectively, increases by 6.93% on MNIST. For the setting of FA-grey, the classification accuracy against clean samples and various attacks is higher than that of FA-white.

G. Comparison between FA and the Other Adversarial Training Methods

To verify that TRADES trained model with FA is more robust than the other adversarial training methods against white-box attacks with weak transferability and black-box attacks,

TABLE VIII

THE ATTACK TIME (MINS) COMPARISON BETWEEN NATURALLY TRAINED DNN MODEL WITH AND WITHOUT FACM ON MNIST, CIFAR10/100. THE LONGER THE ATTACK TIME, THE GREATER THE AMOUNT OF COMPUTATION, AND THE MORE DIFFICULT THE MODEL IS TO BE ATTACKED.

Method	MNIST			CIFAR10			CIFAR100		
	FGSM	PGD40	CW $_{\infty}$	FGSM	PGD20	CW $_{\infty}$	FGSM	PGD20	CW $_{\infty}$
Natural Train	0.03	0.40	2.83	0.07	0.74	9.4	0.17	2.16	25.71
Our FACM	0.21	4.89	33.35	0.35	4.89	71.25	0.29	4.67	70.15

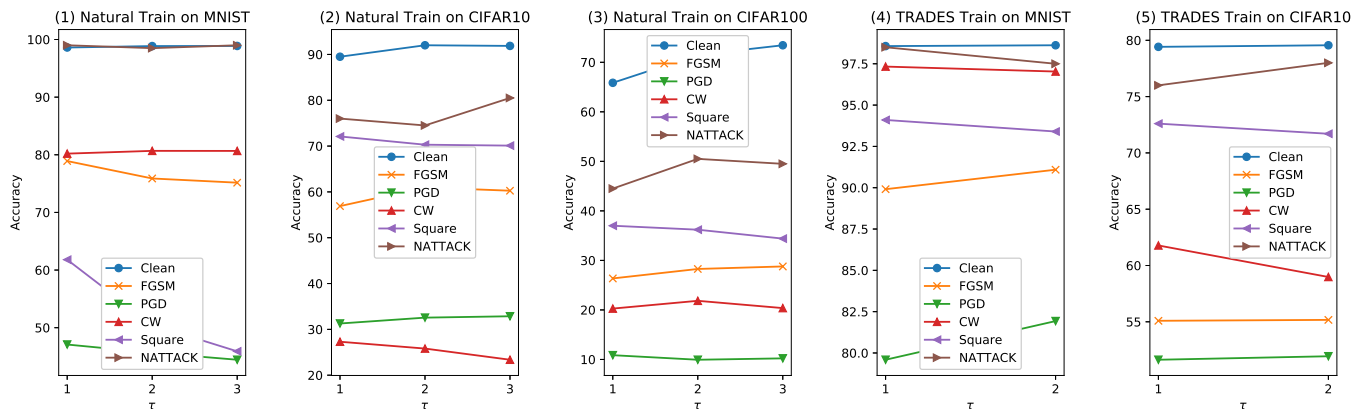


Fig. 15. The influence of the size of the parameter τ on the test accuracy(%) of the FACM-white on MNIST under different types of attacks. In the subgraph (1), the DNN is obtained through natural training; in the subgraph (2), The DNN is obtained through TRADES adversarial training.

TABLE IX

THE INFERENCE TIME (MINS) COMPARISON BETWEEN THE MODEL WITH AND WITHOUT FACM OR FA ON MNIST, CIFAR10 AND CIFAR100.

Method	CIFAR10	CIFAR100	MNIST
TRADES	0.051	0.050	0.028
FA($\tau=2$)+TRADES	0.066	0.068	0.036
FACM($\tau=3$)+TRADES	0.170	0.156	0.052

we compare the classification accuracy of the TRADES trained model with FA and the other six adversarial training methods on CIFAR10/100 and MNIST. As shown in Tables III, IV and V, for the setting of FA-white, the classification accuracy of TRADES with FA is higher than the other six adversarial training methods against the majority white-box attacks with weak transferability and black-box attacks. In comparison with the best one in the other six adversarial training methods, the average improvement is 19.93%, 17.77% and 12.50% on CIFAR10/100 and MNIST, respectively. In addition, for Square, the increase of the attack strength has little impact on the performance of TRADES with FA and has a great impact on the other six adversarial training methods without FA.

H. Comparison between FA and the Channel-wise Activation Suppressing Methods

To further verify that the adversarially trained DNN model with FA is more robust than the channel-wise activation suppressing methods against white-box attacks with weak transferability and black-box attacks, we compare the classification accuracy of TRADES with CAS and TRADES with FA, and CIFS with and without FA on CIFAR10. As shown in Table VI, in comparison with CAS, the classification accuracy of TRADES with FA is higher than that of TRADES with

CAS against various attacks except NATTACK under the slight decrease of performance on clean samples. The average classification accuracy against white-box attacks with weak transferability and black-box attacks increases by 12.3%. In comparison with CIFS, under the slight decrease of performance against clean samples and white-box attacks with good transferability, FA can significantly improve the classification accuracy against white-box attacks with weak transferability and black-box attacks, specifically, the average reduction is slight, i.e. 1.01%, and the average improvement is significant, i.e. 12.64%.

I. The Sensitivity Analysis of τ

Fig 15 investigates the influence of the size of the parameter τ in FACM or FA on the test accuracy of MNIST and CIFAR10/100, respectively. For the naturally trained DNN model with FACM, as the parameter τ becomes larger, the test accuracy of clean samples and NATTACK steadily increase on these three datasets, the test accuracy of the other attacks sometimes increases and sometimes decreases, which depends on the type of dataset. The accuracy of most attacks on the same dataset will increase with the increase of parameter τ . For the adversarially trained DNN model with FA, as the parameter τ becomes larger, the test accuracy of clean samples and white-box attacks with good transferability steadily increase on MNIST and CIFAR10, the test accuracy of white-box attacks with weak transferability and black-box attacks basically decrease on MNIST and CIFAR10.

J. Build Time, Attack Time and Inference Time Comparisons

As shown in Table VII, the build time of the naturally trained DNN model with FACM and the TRADES trained

model with FACM is usually 2.3-4.7 times longer than that without FACM, but it is comparable to some variants of adversarial training. Therefore, the increased build time of FACM is reasonable.

As shown in Table VIII, because the naturally trained DNN model with FACM is equal to an ensemble model, which consists of the naturally trained DNN model itself and all middle layer correction models and all CMPD models, the attack time of the naturally trained DNN model with FACM is 7-12 times longer than that without FACM on MNIST, 5-8 times on CIFAR10 and 1.7-2.7 times on CIFAR100. Therefore, the attack calculation amount of the DNN model with FACM becomes larger, and the attack difficulty becomes larger.

As shown in Table IX, in comparison with the pure model, the inference time of the model with FA has a slight increase. The inference time of the model with FACM is 2-3 times that of the pure model. Although the inference time of the model with FA or FACM increases, the performance of the naturally trained DNN model with FACM and the adversarially trained DNN model with FA is significantly improved.

VI. RELATED WORK

Adversarial Training: Besides several variants of AT have been introduced in Section I, Sriramanan et al. [29] introduced a relaxation term to the standard loss, that finds more suitable gradient-directions, increase attack efficacy and leads to more efficient adversarial training. Wang et al. [30] proposed Once-for-all adversarial training methods with a controlling hyper-parameter as the input where trained model could be adjusted among different standard and robust accuracies at testing time. Stutz et al. [31] tackled the problem of the robustness generalization on the unseen threat model by biasing the model towards low confidence predictions on adversarial examples. Laidlaw et al. [32] developed perceptual adversarial training against a perceptual attack gives robustness against many other types of adversarial attacks. Pang et al. [33] provide comprehensive evaluations on CIFAR10, focusing on the effects of mostly overlooked training tricks and hyperparameters for adversarially trained DNN models.

Robust Architectures: To obtain robust network architectures, Du et al. [34] attempts to trade off exploring diverse structures and exploiting the best structures, and a new stochastic neural networks [35], an intrinsically sparse rewiring approach [36], implicit Euler skip connections [37], LayerCert framework [38], the deep Bayes classifier [39] are proposed to enhance robustness.

Randomness: Randomness is an effective approach to defense black-box attacks. Dhillon et al. [40] proposed stochastic activation pruning, a mixed strategy for adversarial defense. Xie et al. [41] proposed to utilize randomization at inference time to mitigate adversarial effects.

VI. CONCLUSION

In this paper, the middle Feature layer Analysis and Conditional Matching prediction distribution (FACM) model is proposed to improve the model robustness through correcting the output of the DNN with features extracted by middle

layers of DNN. Specifically, we theoretically demonstrate the advantages of FACM in terms of the correction and diversity properties, and empirically justify our FACM on benchmark datasets. The experimental results show that our FACM can effectively improve the robustness of the naturally trained DNN model against various adversarial attacks, especially black-box attacks and white-box attacks with weak transferability. In addition, our FA module can improve the accuracy of the adversarially trained DNN model against both black-box attacks and white-box attacks with weak transferability.

REFERENCES

- [1] Y. Ding, L. Wang, H. Zhang, J. Yi, D. Fan, and B. Gong, "Defending against adversarial attacks using random forest," in *CVPR Workshops*, 2019, pp. 105–114.
- [2] N. Carlini and D. A. Wagner, "Towards evaluating the robustness of neural networks," in *IEEE Symposium on Security and Privacy*, 2017, pp. 39–57.
- [3] S. Moosavi-Dezfooli, A. Fawzi, and P. Frossard, "Deepfool: A simple and accurate method to fool deep neural networks," in *CVPR*, 2016, pp. 2574–2582.
- [4] T. Pang, X. Yang, Y. Dong, T. Xu, J. Zhu, and H. Su, "Boosting adversarial training with hypersphere embedding," in *NeurIPS*, 2020.
- [5] E. Wong, L. Rice, and J. Z. Kolter, "Fast is better than free: Revisiting adversarial training," in *ICLR*, 2020.
- [6] J. Zhang, X. Xu, B. Han, G. Niu, L. Cui, M. Sugiyama, and M. S. Kankanhalli, "Attacks which do not kill training make adversarial learning stronger," in *ICML*, 2020, pp. 11 278–11 287.
- [7] H. Zheng, Z. Zhang, J. Gu, H. Lee, and A. Prakash, "Efficient adversarial training with transferable adversarial examples," in *CVPR*, 2020, pp. 1178–1187.
- [8] D. Zhang, T. Zhang, Y. Lu, Z. Zhu, and B. Dong, "You only propagate once: Accelerating adversarial training via maximal principle," in *NeurIPS*, 2019, pp. 227–238.
- [9] H. Xu, X. Liu, Y. Li, A. K. Jain, and J. Tang, "To be robust or to be fair: Towards fairness in adversarial training," in *ICML*, 2021, pp. 11 492–11 501.
- [10] H. Zhang, Y. Yu, J. Jiao, E. P. Xing, L. El Ghaoui, and M. I. Jordan, "Theoretically principled trade-off between robustness and accuracy," in *ICML*, 2019, pp. 7472–7482.
- [11] Y. Bai, Y. Zeng, Y. Jiang, S. Xia, X. Ma, and Y. Wang, "Improving adversarial robustness via channel-wise activation suppressing," in *ICLR*, 2021.
- [12] H. Yan, J. Zhang, G. Niu, J. Feng, V. Y. F. Tan, and M. Sugiyama, "CIFs: improving adversarial robustness of cnns via channel-wise importance-based feature selection," in *ICML*, 2021, pp. 11 693–11 703.
- [13] A. Madry, A. Makelov, L. Schmidt, D. Tsipras, and A. Vladu, "Towards deep learning models resistant to adversarial attacks," in *ICLR (Poster)*, 2018.
- [14] G. Vacanti and A. V. Looveren, "Adversarial detection and correction by matching prediction distributions," *CoRR*, vol. abs/2002.09364, 2020.
- [15] Z.-H. Zhou, "Computational learning theory," in *Machine Learning*, 2021, pp. 287–313.
- [16] S. Ma, Y. Liu, G. Tao, W. Lee, and X. Zhang, "NIC: detecting adversarial samples with neural network invariant checking," in *NDSS*, 2019.
- [17] W. Wu, Y. Su, X. Chen, S. Zhao, I. King, M. R. Lyu, and Y. Tai, "Boosting the transferability of adversarial samples via attention," in *CVPR*, 2020, pp. 1158–1167.
- [18] Y. LeCun, C. Cortes, and C. Burges, "Mnist handwritten digit database," *ATT Labs [Online]*. Available: <http://yann.lecun.com/exdb/mnist>, vol. 2, 2010.
- [19] A. Krizhevsky, "Learning multiple layers of features from tiny images," 2009.
- [20] N. Papernot, P. D. McDaniel, X. Wu, S. Jha, and A. Swami, "Distillation as a defense to adversarial perturbations against deep neural networks," in *IEEE Symposium on Security and Privacy*, 2016, pp. 582–597.
- [21] S. Zagoruyko and N. Komodakis, "Wide residual networks," in *BMVC*, 2016.
- [22] I. J. Goodfellow, J. Shlens, and C. Szegedy, "Explaining and harnessing adversarial examples," in *ICLR (Poster)*, 2015.
- [23] A. Madry, A. Makelov, L. Schmidt, D. Tsipras, and A. Vladu, "Towards deep learning models resistant to adversarial attacks," in *ICLR (Poster)*, 2018.

- [24] Y. Dong, F. Liao, T. Pang, H. Su, J. Zhu, X. Hu, and J. Li, “Boosting adversarial attacks with momentum,” in *CVPR*, 2018, pp. 9185–9193.
- [25] F. Croce and M. Hein, “Reliable evaluation of adversarial robustness with an ensemble of diverse parameter-free attacks,” in *ICML*, 2020, pp. 2206–2216.
- [26] M. Andriushchenko, F. Croce, N. Flammarion, and M. Hein, “Square attack: A query-efficient black-box adversarial attack via random search,” in *ECCV (23)*, 2020, pp. 484–501.
- [27] Y. Li, L. Li, L. Wang, T. Zhang, and B. Gong, “NATTACK: learning the distributions of adversarial examples for an improved black-box attack on deep neural networks,” in *ICML*, 2019, pp. 3866–3876.
- [28] Adversarial-Attacks-PyTorch. [Online]. Available: <https://github.com/Harry24k/adversarial-attacks-pytorch>
- [29] G. Sriramanan, S. Addepalli, A. Baburaj, and V. B. R., “Guided adversarial attack for evaluating and enhancing adversarial defenses,” in *NeurIPS*, 2020.
- [30] H. Wang, T. Chen, S. Gui, T. Hu, J. Liu, and Z. Wang, “Once-for-all adversarial training: In-situ tradeoff between robustness and accuracy for free,” in *NeurIPS*, 2020.
- [31] D. Stutz, M. Hein, and B. Schiele, “Confidence-calibrated adversarial training: Generalizing to unseen attacks,” in *ICML*, 2020, pp. 9155–9166.
- [32] C. Laidlaw, S. Singla, and S. Feizi, “Perceptual adversarial robustness: Defense against unseen threat models,” in *ICLR*, 2021.
- [33] T. Pang, X. Yang, Y. Dong, H. Su, and J. Zhu, “Bag of tricks for adversarial training,” in *ICLR*, 2021.
- [34] X. Du, J. Zhang, B. Han, T. Liu, Y. Rong, G. Niu, J. Huang, and M. Sugiyama, “Learning diverse-structured networks for adversarial robustness,” in *ICML*, 2021, pp. 2880–2891.
- [35] P. Eustratiadis, H. Gouk, D. Li, and T. M. Hospedales, “Weight-covariance alignment for adversarially robust neural networks,” in *ICML*, 2021, pp. 3047–3056.
- [36] O. Özdenizci and R. Legenstein, “Training adversarially robust sparse networks via bayesian connectivity sampling,” in *ICML*, 2021, pp. 8314–8324.
- [37] M. Li, L. He, and Z. Lin, “Implicit euler skip connections: Enhancing adversarial robustness via numerical stability,” in *ICML*, 2020, pp. 5874–5883.
- [38] C. H. Lim, R. Urtasun, and E. Yumer, “Hierarchical verification for adversarial robustness,” in *ICML*, 2020, pp. 6072–6082.
- [39] Y. Li, J. Bradshaw, and Y. Sharma, “Are generative classifiers more robust to adversarial attacks?” in *ICML*, 2019, pp. 3804–3814.
- [40] G. S. Dhillon, K. Azizzadenesheli, Z. C. Lipton, J. Bernstein, J. Kossaifi, A. Khanna, and A. Anandkumar, “Stochastic activation pruning for robust adversarial defense,” in *ICLR (Poster)*, 2018.
- [41] C. Xie, J. Wang, Z. Zhang, Z. Ren, and A. L. Yuille, “Mitigating adversarial effects through randomization,” in *ICLR (Poster)*, 2018.